

# The structural connectome in children: basic concepts, how to build it, and synopsis of challenges for the developing pediatric brain

Avner Meoded<sup>1</sup> · Thierry A. G. M. Huisman<sup>2</sup> · Maria Grazia Sacco Casamassima<sup>3</sup> · George I. Jallo<sup>3</sup> · Andrea Poretti<sup>2</sup>

Received: 30 August 2016 / Accepted: 22 March 2017 / Published online: 5 April 2017  
© Springer-Verlag Berlin Heidelberg 2017

## Abstract

**Purpose** The structural connectome is a comprehensive structural description of the network of elements and connections forming the brain. In recent years, this framework has progressively been used to investigate the pediatric brain.

**Methods** We discuss the different steps and emphasize key technical aspects required for the successful reconstruction, analysis, and visualization of the pediatric structural connectome using current state-of-the-art neuroimaging and post-processing techniques.

**Results** The two key components of structural connectome are a node (a cortical region obtained with high-resolution anatomical imaging) and an edge (structural association between cortical regions, defined with tractography). After delineation of nodes and edges, an association matrix can be generated by compiling all pairwise associations between nodes and applying a threshold to produce a binary adjacency matrix. Several measures can be used to characterize the topological architecture of the brain's networks. Finally, we provide an overview of various visualization methods of the structural connectome in children.

**Conclusion** The human connectome is the culmination of more than a century of conceptual and methodological innovation. Biological substrates of brain development such as cortical gyration and myelination challenge the acquisition, reconstruction, and analysis of structural connectome in children and require specific considerations compared to adults.

**Keywords** Diffusion tensor imaging · Structural connectome · Tractography · Brain · Children

## Introduction

Connectomics based on graph theory has become a unique methodological framework for studying structural connectivity patterns of the pediatric brain. The term “connectome” embodies the advances of over a century of neuroscientific innovation and reflects the agenda for a new era: the era of the brain networks [1]. The complex network approach to neuroimaging represents a conceptual revolution, not just an evolution of existing techniques. The human connectome is the comprehensive structural description of the network of elements and connections forming the human brain and can be mathematically described as a neural graph [2–4]. Brain graphs provide a relatively simple and increasingly popular way of modeling the human brain connectome, using graph theory to abstractly define the brain as a set of anatomical regions, the so-called *nodes*, and structural connections, the so-called interconnecting *edges* [4, 5].

The main impact of graph theory is to promote a change of perspective in how we look at the brain [6]. The connectome provides a unified, time-invariant, and readily available neuroinformatics resource that can be used in virtually all areas of experimental and theoretical neuroscience [7]. Network analyses of brain connectivity have begun to yield

---

✉ Avner Meoded  
ameoded1@jhmi.edu

<sup>1</sup> Department of Radiology, Johns Hopkins All Children's Hospital, The Johns Hopkins University School of Medicine, 501 6th Avenue South, St. Petersburg, FL 33701, USA

<sup>2</sup> Section of Pediatric Neuroradiology, Division of Pediatric Radiology, Russell H. Morgan Department of Radiology and Radiological Science, The Johns Hopkins University School of Medicine, Baltimore, MD, USA

<sup>3</sup> Johns Hopkins All Children's Institute for Brain Protection Sciences, St. Petersburg, FL, USA

important insights into brain organization of humans and non-human primates [8]. Network measures are critical for creating metrics that allow the comparison of connectivity patterns across individuals and imaging modalities, as well as clinical conditions. Graph measures allow the characterization of network structure by identifying local contributions of individual nodes and connections, as well as the network's global capacity to integrate information, or its tendency to form interconnected communities or modules [9]. Complex network properties have been identified with some consistency in all modalities of neuroimaging data and over a range of spatial and time scales. Conserved properties include small worldness, high efficiency of information transfer for low wiring cost, modularity, and the existence of network hubs [10–12]. In recent years, this framework has been used to investigate the pediatric brain. Normal brain development is characterized by continuous and significant network evolution throughout infancy, childhood, and adolescence, following specific maturational steps. Uncovering these complex processes is crucial to understanding the development of brain networking. With the recent advancement of noninvasive neuroimaging techniques to study the pediatric brain, the comprehensive macroscale connectome can be evaluated in children in vivo.

Currently, various neurodevelopmental disorders, such as autism spectrum disorder, attention-deficit hyperactivity disorder, and schizophrenia, some congenital malformations and traumatic brain injury may be considered as connectopathies or disconnection syndromes, and thus, the structural connectome may help us understand the pathogenesis and implication for cognitive and behavioral functions of brain disorders from a network perspective [13–19].

Among the imaging modalities used for macroconnectomics, magnetic resonance imaging (MRI) is dominant, partly because of widespread availability, safety, and spatial resolution. Diffusion weighted (DWI) and diffusion tensor imaging (DTI) as well as functional MRI (fMRI) are widely used for inferring structural and functional connectivity. Several important steps are needed for the reconstruction of the structural connectome. First, a morphological high-resolution T1-weighted MRI is used to segment the brain and identify cortical regions, e.g., nodes. Second, the macroscopic pathways of the underlying neuronal fibers need to be estimated from DWI/DTI by means of tractography, namely edges. Subsequently, the connectivity matrix is obtained by associating edges between each pairs of nodes. Finally, sophisticated methods of connectome visualization are used for network representation. In each of these steps, there are many important parameters that can lead to variations of the connectomes depending on how they are calibrated.

In this review article, we focus on the up-to-date mapping, description, and analysis pipelines of macroscale pediatric structural connectome. We first review approaches and challenges to segment the developing brain into discrete nodes and then discuss the imaging and analytic methodologies used to

map and quantify patterns of structural connectivity that are represented by edges in the connectome. For each step of the structural connectome reconstruction, we included special considerations for the pediatric population highlighting challenges and discussing potential limitations related to the pediatric brain that are different compared to the structural connectome reconstruction in adults.

## The ingredients of structural connectome

The two key components required for structural connectome reconstruction are a *node* and an *edge*. Nodes correspond to neuronal elements, e.g., gray matter voxels or brain regions. For this purpose, high-resolution T1-weighted MRI is needed. Edges represent measures of structural association between cortical regions and are derived from DTI tractography. The results of the structural connectome reconstruction depend on the quality of the acquired imaging data. For a precise reconstruction of the structural connectome, high-resolution T1-weighted MRI and DTI are required. Ideally, high-resolution DTI data should be acquired at high field strength along multiple noncollinear directions (30 or more) and with multiple *b* values [20].

## Defining nodes—cortical parcellation

Defining the nodes of a macroscale connectome is a complex task as there is lack of agreement on how best to define the different cortical regions. Parcellations of the brain into different nodes should (1) be distinct in that each brain segment only belongs to one region, (2) assign tissue to one node that has similar connections to other parts of the brain, and (3) only be compared with other networks that use the same parcellation scheme. The goal is to segment the cortex in a standard way such that regions of interest (ROI) are robustly placed on the same cortical surface across subjects, enabling the construction of whole brain normalized connection matrix at multiple scales, which can be averaged and compared over population of subjects [21].

Different parcellations of the human brain exist. Atlases of brain areas generated using anatomical and functional parcellation schemes are available (Fig. 1) [1]. In children, the accurate identification of cortical regions at high resolution is challenging because sulci continue to develop after birth resulting in a rapidly changing complexity of the brain surface/sulci. In addition, the MRI contrast in the brain of young children varies considerably with age, and it is not always straightforward to delineate what constitutes a normal appearance and what degree of variability reflects a pathological condition. Template-based volumetric registration like in statistical parametric mapping (SPM) software and Montreal

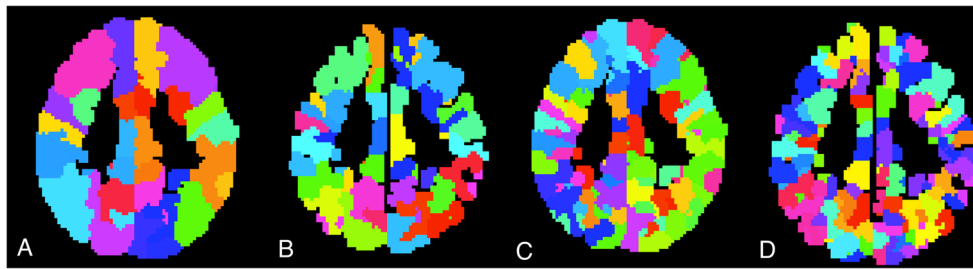


**Fig. 1** Different parcellations of the human brain. Atlases of brain areas generated using anatomical parcellation schemes. **a** Lausanne2008 atlas with 66 cortical regions—also known as the Desikan-Killiany atlas. **b**

Lausanne2008 atlas with 120 cortical regions. **c** Lausanne2008 atlas with 250 cortical regions. **d** Lausanne2008 atlas with 500 cortical regions

neurological institute (MNI) space or surface-based matching like in Freesurfer (<http://surfer.nmr.mgh.harvard.edu>) has shown great results in adults and older children [22]. The adult brain templates and in adults widely used software life Freesurfer, however, do not work with incompletely myelinated brain. [23] For pediatric brain analysis, attempts have been made to create age-specific brain templates. Multi-contrast, single-subject atlases for neonates and 18-month-old as well as 2-year-old children have been recently developed. [24] The low gray matter/white matter contrast in both T1- and T2-weighted MR images in young children compared to the adult brain, however, makes the accurate normalization of one brain to another very difficult [24]. A template-free parcellation that uses unconstrained parcellation schemes and enables calculation of single-subject network parameters without imposing anatomical bias may be a valuable alternative and has shown promising results in the segmentation of the neonatal brain [25].

A novel data-driven approach to explore the cortical architecture has been recently described such as Dense Individualized and Common Connectivity-based Cortical Landmarks (DICCCOLs). This approach allows to effectively represent the common cortical architecture by groupwise consistent structural fiber connections without the need to acquire high-resolution T1-weighted images for cortical parcellation [26].

### Defining edges—structural connectivity

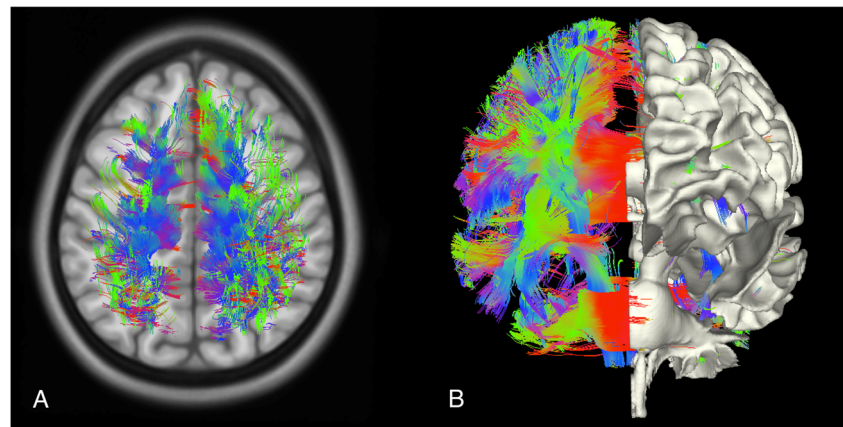
After defining the nodes as anatomically distinct brain regions, the next step of the connectome reconstruction includes the evaluation of the structural connectivity by measuring interregional fiber tracks. Tractography is the most commonly used diffusion DWI/DTI method for defining structural connectivity. Briefly, DWI/DTI exploits the principles of traditional MRI to measure the random motion of water molecules and subsequently to (1) infer information about white matter microstructural properties and (2) delineate the gross axonal organization of the brain. White matter is characterized by bundles of myelinated axons surrounded by myelin sheaths that are built up by layers of membranes. This restricts

diffusion of free water molecules; i.e., the myelin layers and the axonal membrane cause a lower restriction parallel than perpendicular the axon and thus a higher anisotropy [27]. The main technique by which individual structural connectome reconstruction is made possible in vivo is DWI/DTI. To date, DTI tractography is still the only in vivo tool capable of estimating structural connectivity in the brain. The basic principle underlying the inference of structural connectivity from diffusion MRI data is that water diffusion in white matter is hindered and occurs primarily along the path of axons. By following the motion of water, it is possible to map the orientation(s) of fibers passing through each voxel of white matter [1]. Fiber tractography is a rendering method for improving the depiction of data from DWI/DTI of the brain (Fig. 2) [28–33].

The primary purpose of tractography is to clarify the orientational architecture of tissues by integrating pathways of maximum diffusion coherence. The fibers depicted with tractography are often considered to represent axonal bundles or nerve fibers, but they are more correctly viewed in physical terms as lines of fast diffusion that follow the local diffusion maxima and that only generally reflect the axonal architecture [34]. Fiber orientation must be inferred for white matter voxels individually, before any connectivity analysis. The goal of DWI/DTI analysis is to infer a probability function for each voxel, which captures the different fiber orientations present and their relative proportions. Estimation of this function at each voxel, which is referred to as the fiber orientation density function (fODF), is the first step in estimating structural connectivity (Fig. 3).

The DTI model performs well in regions where there is only one fiber population (i.e., fibers are aligned along a single axis), where it gives a good depiction of the fiber orientation. However, this is not always the case. Fibers are known to disperse (fan), cross, merge, and kiss (temporarily run adjacent to one another), all of which can occur within the same single voxel and lead to heterogeneity not accounted for by a simple delta function. Complex fODF models better estimate fiber trajectories, particularly when several white matter tracts intersect and allow recovery of nondominant pathways invisible to DTI. Imaging techniques that provide higher angular

**Fig. 2** **a** 3D depiction of whole brain tractography obtained with HARDI of an 8-year-old healthy subject overlaid on high-resolution axial T1WI. **b** Coronal view of whole brain tractography with hemi-brain surface. Improved tractography with HARDI is capable of capturing more connections and yields detailed representation of the white matter



resolution are needed [35, 36]. Two newer types of diffusion imaging, diffusion spectrum imaging (DSI) and high-angular resolution diffusion imaging (HARDI), and their variations have begun to replace DTI in recent years. Although they differ in their details, HARDI and DSI ultimately work by detecting the movement of water in many more directions within a given voxel. DSI can overcome this limitation by reconstructing multiple diffusion directions in each voxel [37].

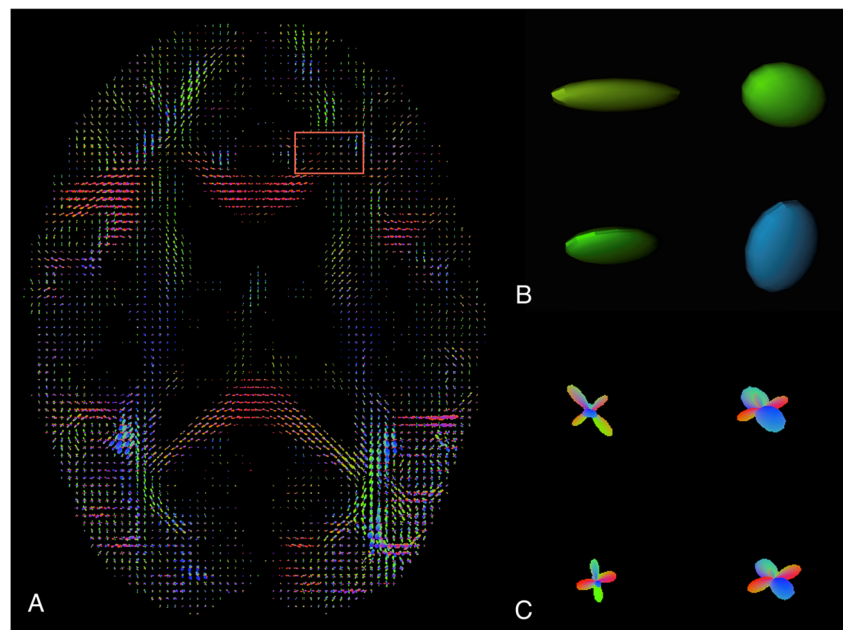
After estimation of the fODF in each voxel, tractography approaches such as deterministic or probabilistic are used to establish structural connectivity between connectome nodes. With deterministic tractography, 3D trajectories, e.g., “streamlines”, are used to trace putative white matter paths. The individual streamlines do not represent actual axons; they depict estimates of the average trajectories of axon bundles, given our assumption that diffusion is least hindered along axons [1]. However, streamlines tractography suffers from a

number of inherent limitations, one of which is the accurate determination of when streamlines should be terminated. “Anatomically constrained tractography” improves tractography through effective use of anatomical information and prevents spurious streamline terminations for improved connectome reconstruction [38].

With probabilistic tractography, it is possible to assign a probability of axonal connection between any pair of gray matter regions on the basis of tractographic analysis of an individual dataset. For DTI, DSI, or HARDI dataset of a subject, probabilistic tractography allows to assign a probability of axonal connection, while deterministic tractography reconstructs the “number of axons” between any pair of gray matter regions. In this way, the “connection” between each pair of cortical regions in the brain can be quantified [23, 34, 35, 37, 39].

Special considerations for children deserve to be mentioned here. First, the duration of a high-resolution DWI/DTI protocol is challenging for children. Currently, the main

**Fig. 3** **a** Axial view of DTI fiber orientation estimates. The *zoomed area* represents one of the most critical “cross-roads” of the human brain: the region where corpus callosum, corona radiata, and superior longitudinal fasciculus fibers intersect. **b** Tensor ellipsoid. **c** fODF: note how fODF better estimate fiber trajectories and allow recovery of nondominant pathways invisible to DTI



human connectome project (HCP) protocol lasts approximately 60 min for DWI/DTI acquisition, which is very long for young children and difficult to obtain without sedation. Lifespan-HCP protocol implemented a pilot protocol and settled on a modified 20 min DWI/DTI protocol. In addition, the collaboration with a child life specialist may improve child compliance with MRI and hence reduce the problem of motion and the difficulty of performing longer scans in children. The MRI scans are acquired in pairs with opposing phase-encoding polarity, which increases the signal-to-noise ratio (SNR) and allows corrections of susceptibility-induced and eddy current-induced distortions (see <http://lifespan.humanconnectome.org>) [40, 41]. Second, the measurement of the development of brain connectivity is very challenging and is prone to mis-interpretation. In the maturing brain, diffusion anisotropy changes physiologically, which also directly affects tractographic results. The low fractional anisotropy (FA) in the unmyelinated white matter hampers traditional tractography approaches in the developing brain [23]. Moreover, the patient weight has been shown to affect the incidence of mechanical vibration-induced artifact, making children potentially more susceptible than adults [42]. This has important implications for the interpretation of the results of longitudinal DWI/DTI studies. Visual inspection remains the primary method for artifact identification in such cases. In addition, other artifacts such as those originating from cardiac pulsation in ungated acquisitions and those originating from subject motion when scanning uncooperative patients or unsedated pediatric subjects may decrease data quality. Different automated algorithms have been developed for data analysis and correction. One novel approach for robust diffusion tensor estimation, called RESTORE (robust estimation of tensors by outlier rejection) uses iteratively reweighted least-squares regression to identify potential outliers and subsequently exclude them. This has been shown to improve tensor estimation [43].

Furthermore, assessing the anatomical accuracy of tractography is difficult because of the lack of independent knowledge of the true anatomical connections in humans. There is an inherent limitation in determining long-range anatomical projections based on voxel-averaged estimates of local fiber orientation obtained from DWI/DTI data that is unlikely to be overcome by improvements in data acquisition and analysis alone [44]. Last but not least, the accuracy and reproducibility of constructing the structural connectome done with different acquisition and reconstruction techniques are not well defined. To date, there is limited consensus on what the reference method for structural connectome tractography should be.

All diffusion schemes, from the classical DTI to the high-angular resolution DSI, produce a biologically meaningful mapping of the human connectome. However, different tractography algorithms can influence the estimation of several network indices that characterize the human structural

connectome such as differences in network topology. It is important to note that the findings of small worldness, high global network efficiency, and high density hubs per se, characteristic for the human brain, are very robust over all investigated methods and parameters [45–47].

### The matrix

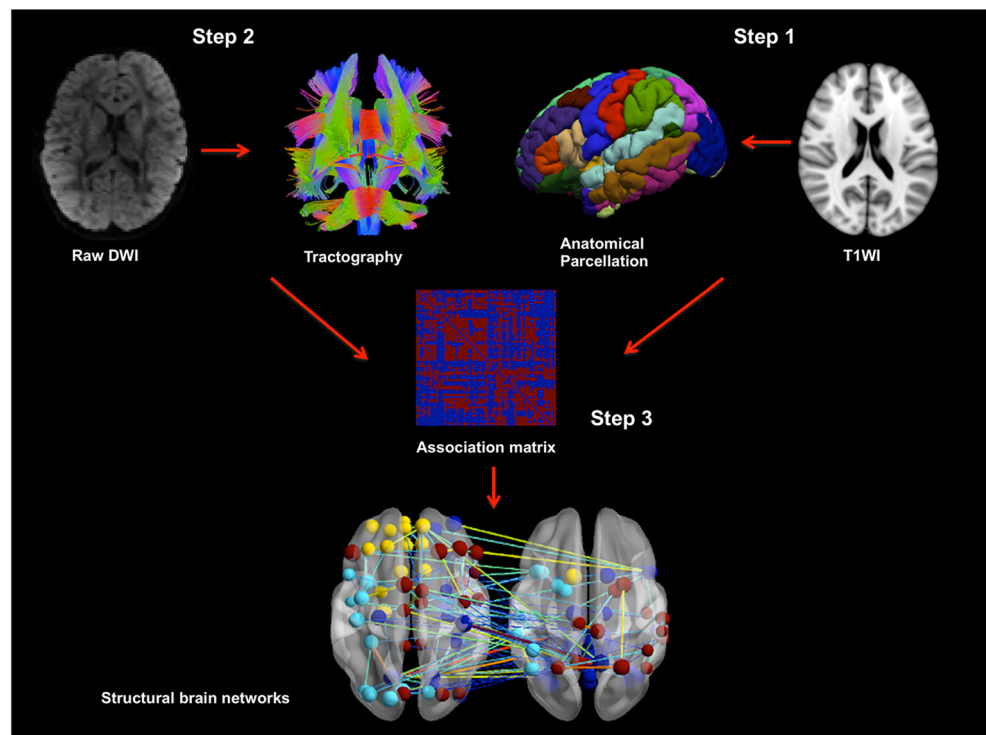
The next step in structural connectome reconstruction is the generation of an association matrix by compiling all pairwise associations between nodes. By applying a threshold to each element of this matrix, we obtain a binary adjacency matrix or undirected graph. There are many possibilities to identify the threshold for connectivity matrices (e.g., FA or  $1/\text{apparent diffusion coefficient}$ ) and it is a focus of ongoing studies to determine whether a thresholding is needed and, if yes, which one is the most accurate. An adjacency matrix indicates the number of edges between each pair of nodes in a graph. For most brain networks, the adjacency matrix is specified as binary. This means that each element is either 1 (if there is an edge between nodes) or 0 (if there is no edge). For undirected graphs, the adjacency matrix is symmetrical [3].

Edges are differentiated on the basis of their weight and directionality. Network edges may be directed (drawn as arrows) or undirected (drawn as lines). A directed edge makes a claim about the causal relations between nodes, whereas an undirected edge is agnostic about causality. In human neuroimaging data, it is currently more difficult to assign directionality to associations between regions, whether measured by structural MRI, DTI, DSI, or fMRI. Although the majority of network studies of neuroimaging data have been performed on binary or unweighted networks, in which each edge has a weight of one and each nonedge has a weight of zero, there has been a growing interest in the use of weighted networks that contain information about connection strengths [4, 48]. After completing the connectome reconstruction, it is possible to calculate the network parameters of interest in this graphical model of a brain network (Fig. 4).

### The metrics—topology measures

Because network analysis is based on the mathematical field of graph theory, there is a wide variety of measures that can be used to characterize the topological architecture of the brain's anatomical or functional connectivity. In particular, graphs are commonly assessed in terms of their local and global connectivity/efficiency (Table 1) [48]. The interpretation of topology measures in young children may be different compared to adults. For example, changes in measures of integration and segregation have been shown with brain maturation and ongoing myelination [49]. Normal brain development is

**Fig. 4** 4-year healthy boy structural brain connectome, explored using graph theory through the following steps: (1) *step 1*: define the network nodes, with anatomical parcellation of high-resolution T1WI, (2) *step 2*: estimate a continuous measure of association between nodes with structural connectivity, obtained with tractography, and (3) *step 3*: generate an association matrix by compiling all pairwise associations between nodes. The result of these three steps is the structural connectome, a graphical model of a brain network



characterized by continuous network development/changes from infancy, throughout childhood, and adolescence, following specific maturational patterns. During development, the structural connectome demonstrates increased global integration and robustness and decreased local segregation, as well as strengthening of the hubs. This suggests that progressive white matter myelination favors increased global efficiency [22]. This age-dependent maturation of the structural connectome warrants separate analysis of graphs of partially myelinated (<2 years old) and fully myelinated brains (>2 years old). Network measures can be used as diagnostic biomarkers to quantify differences between patients and healthy subjects. Network measures have been reported to be altered in several neuropsychiatric developmental disorders, such as autism spectrum disorders or attention-deficit hyperactivity disorder [50]. Neuroimaging studies on structural connectome during development and pediatric CNS disease are included in Table 2.

### Measure of local connectivity

The clustering coefficient is a measure of local segregation or efficiency. It measures the density of connections between the node neighbors. Densely interconnected neighbors form a cluster around the node. Transitivity is a normalized variant of clustering coefficient that is not influenced by nodes with low degree of connections [11]. Networks with a high level of clustering are often composed of local communities or modules of densely interconnected nodes where most edges link

nodes within modules and few edges link nodes between modules. Modularity indicates a decomposability of the system into smaller subsystems, e.g., community structure, and is revealed by partitioning the network into groups of nodes, with a maximally possible number of within-group links and a minimally possible number of between-group modular networks that are composed of topological modules or communities [68]. The degree to which the network may be partitioned into such clearly delineated and nonoverlapping groups is quantified by a single statistic, the modularity [69].

### Measures of global connectivity

Paths are sequences of distinct nodes and edges and in anatomical networks represent potential trajectory of information flow between pairs of brain regions.

Characteristic path length is a measure of a network integration and is calculated as the average shortest path length between all pairs of nodes in the network. In general, each node can be reached from any other node along a path composed of only a few edges. Short paths are likely to be the most effective for internode communication [11]. The average inverse shortest path length is a related measure known as the global efficiency [10].

### Measures of influence and centrality

The degree (strength) is a basic and important measure of a network. The degree of a node is the number of edges

**Table 1** Structural connectome glossary

Network measure	Definition
<b>Measures of local connectivity</b>	
Clustering coefficient	A measure of local segregation or efficiency measures the density of connections between the node's neighbors
Transitivity	A normalized variant of clustering coefficient not influenced by nodes with low degree
Modularity	Decomposability of the system into smaller subsystems, e.g., community structure
<b>Measures of global connectivity</b>	
Characteristic path length	A measure of network integration is the average shortest path length between all pairs of nodes in the network; short paths are likely to be the most effective for internode communication
<b>Measures of influence and centrality</b>	
Degree	Number of edges connecting it to the rest of the network
Hub	Important nodes highly connected to the rest of the network facilitate global integrative processes
Betweenness centrality	Fraction of all the shortest paths in the network that pass through the node
<b>Measures of resilience</b>	
Degree distribution	The distribution of degrees over all nodes in the network; brain graphs typically have a broad-scale degree distribution, implying that at least a few “hubs” will have high degree
Assortativity coefficient	Measure of resilience and is the correlation coefficient for the degree of neighboring nodes; networks with a positive assortativity coefficient are resilient. Networks with a negative assortativity are likely vulnerable
<b>Other</b>	
Small worldness	The combination of high clustering and short characteristic path length; also defined as the combination of high global and local efficiency of information transfer between nodes of a network

connecting it to the rest of the network. Hubs are important nodes that are more highly or densely connected to the rest of the network, facilitate global integrative processes, or play critical compensatory role when a network is damaged (node with high degree/betweenness centrality). Various measures of centrality are based on the idea that central nodes participate in many short paths within a network and consequently act as important controls of information flow [70, 71]. Betweenness centrality is the fraction of all the shortest paths in the network that pass through the node. A node with high betweenness centrality can control information flow because it represents

the intersection of many short paths. Centrality measures identify elements that are highly interconnected or carry a significant proportion of signal traffic.

### Measures of resilience

The distribution of degrees over all nodes in the network can be described as a degree (probability) distribution. Brain graphs typically have a broad-scale degree distribution. This implies that at least a few “hub” nodes will have high degree and interact with large number of other nodes. The mean network degree is most commonly used as a measure of density or the total “wiring cost” of the network [48]. The assortativity coefficient is a correlation coefficient for the degree of neighboring nodes. Networks with a positive assortativity coefficient are therefore likely to have a comparatively resilient core of mutually interconnected high-degree hubs. On the other hand, networks with a negative assortativity coefficient are likely to have widely distributed and consequently vulnerable high-degree hubs [72]. Small worldness has been originally defined as the combination of high clustering and short characteristic path length. Recently, this definition has been modified to the combination of high global and local efficiency of information transfer between nodes of a network [73]. A well-designed anatomical network could therefore reconcile the presence of functionally specialized (segregated) modules with a robust number of intermodular (integrated) edges. Small worldness appears to be a ubiquitous organization of anatomical connectivity [73–75].

### Comparison of graphs

When comparing brain graphs and topology measures, it is important to observe two main rules: the graphs to be compared must have (i) the same number of nodes and (ii) the same number of edges. This is because the quantitative values of topological metrics will depend on both the size and connection density of the graphs [4]. Furthermore, building “consensus connectomes” are necessary when analyzing heterogeneous group of subjects with too much interindividual variation of structural connectivity. The consensus connectomes have the advantage of being pooled across all the individuals in the group, which smooths out individual variation and allows for comparison of graph metrics with other studies that have reported results for consensus connectomes [14]. This method has been recently applied in children with segmental callosal agenesis [19]. In addition to comparing topological structures of entire graphs, we can identify subnetworks of graphs that are different between groups, e.g., network-based statistics (NBS) [76]. NBS has the ability to detect differences in connectivity between

**Table 2** Neuroimaging studies on structural connectome during development and pediatric CNS disease

Study	Study purpose	Study population	Number	Age at scan Mean $\pm$ SD (range) Gender M/F	Findings
Pandit et al. [51]	Identifying patterns and strength of connectivity following premature birth	Preterm-born children (median GA at birth 28.29 weeks)	49	13 m <sup>a</sup> (11–16 m) 25 m <sup>a</sup> (23.5–31.5 m) M/F, 23/26	Connection strength $\downarrow$ in tract involving cortical and subcortical structure
Grayson et al. D.S. [52]	Comparing structural and functional rich club organization across age	Children and adults	29 Children, 15 Adults, 14	(7–11 years); M/F, 8/7 (24–35 years); M/F, 4/10	No differences in general architecture of rich club between children and adults Rich club organization of functional networks $\uparrow$ across age
Kim Dea-Jin et al. [53]	Investigate the effects of gestational length on the structural network organization at preadolescent age	Preadolescents	147 <sup>b</sup> Preterm-born, 48 (GA at birth 33.3 $\pm$ 2.6 weeks) Term-born, 99 (GA at birth 39.25 $\pm$ 1.29 weeks)	8.12 $\pm$ 1.35 years (6–11 years) M/F, 81/66	Higher network efficiency associated with longer gestation
Yap P.-T. et al. [54]	Characterize brain network connectivity in the 1st year of life Longitudinal study	Infants and toddlers	39	2-week-olds (GA 41.6 $\pm$ 1.7 weeks) 1-year-olds (94.2 $\pm$ 2.3 weeks) 2-year-olds (145.2 $\pm$ 4.8 weeks) M/F, 18/21	Small world at birth with increased efficiency in later stages of development.
Huang H. et al. [55]	Evaluate structural basis of the development of functional networks	Neonates Toddlers Preadolescents	63 Neonates, 25 Toddlers, 13 Preadolescents, 25	GA 39.5 $\pm$ 2.3 weeks (37–43 weeks) M/F, 13/12 2.3 $\pm$ 0.5 years (1.8–3.1 years) M/F, 8/5 11.8 $\pm$ 1.8 years (10.7–13.5 years) M/F, 13/12	Monotonic increase of network efficiency and strength through infancy and childhood
Baker S.T.E. [56]	Mapping longitudinal changes in structural connectivity during late adolescence	Adolescents	31 <sup>b</sup>	1st scan, 16.6 $\pm$ 0.5 years (15.6–17.9 years) 2nd scan, 18.9 $\pm$ 0.5 years (17.9–19.9 years) M/F, 18/13	Selective remodeling of hub-hub connectivity with shifting from subcortical to frontal hub regions
Wierenga L.M. et al. [57]	Describe regional patterns of age-related changes within white matter and explore developmental patterns in global network topology	Childhood to early adulthood	123 Dataset I, 85 Dataset II, 38 (for independent replication)	(7–22.6 years) M/F, 53/32 (7.4–22.9 years) M/F, 23/15	Age-related decrease in average path length, increase in node strength, and network clustering
Ball G. et al. [58]	Determine whether environmental factors can affect network brain development Longitudinal study	Preterm and term-born infants	63 Preterm, 46 <sup>c</sup> Term-born, 17	Median age at 2nd scan, 41 weeks Preterm: M/F, 22/24 Term-born: M/F, 6/11	Premature exposure to the extrauterine environment is associated with altered network



**Table 2** (continued)

Study	Study purpose	Study population	Number	Age at scan Mean ± SD (range) Gender M/F	Findings
Zhao T. et al. [59]	Provide a complete view of the topological changes of the structural connectome over age	Lifespan	113 <sup>b</sup>	38.2 ± 21.4 years (9–85 years) M/F, 63	architecture and reduced network capacity Disruption in both cortical-subcortical connectivity and short distance cortico-cortical connections u-shaped trajectory with a peak around the third decade of global network property
Chen Z. et al. [60]	To map the developmental changes of the structural brain network	Early childhood to adulthood (age range 6–30 years)	180 <sup>b</sup> Early childhood, 36 Late childhood, 36 Adolescents, 36 Young adults, 36 Adults, 36	8.1 ± 1.1 years (6–9.8 years); M/F, 16/20 11.6 ± 0.9 years (9.9–12.7 years); M/F, 19/17 15.4 ± 1.4 years (12.9–17.9); M/F, 15/21 19.4 ± 1.1 years (17.6–21.8 years); M/F, 18/18 25.7 ± 2.7 years (21.9–29.7 years); M/F, 16/20 9.9 ± 1.4 years 1st scan 12.9 ± 1.4 years 2nd scan	↑ in global efficiency and ↓ in modularity in late childhood
Koenis M.M.G. et al. [61]	To map global and local efficiency of structural brain networks in twin and sibling adolescents Longitudinal study	Early adolescence	162 Monozygotic twin, 57 Dizygotic twin, 63 Older siblings, 42		FA-based local and global efficiency ↑ during early adolescence. Increase in FA-based network efficiency and decreases in streamline count based local efficiency are related to increases in intellectual functioning
Hagmann P. et al. [22]	To explore the contribution of white matter maturation to the development of connectivity between ages 2 to 18 years	Toddlers Children Adolescents	30	Age range 18 months–18 years	Major structural modules and hubs are seen by 2 years of age with continued strengthening during development. ↑global efficiency, ↓clustering and small worldness
Tymofiyeva O. et al. [62]	To evaluate maturational changes of the cortical connectome across the age spectrum from premature to adults	Preterm to adults	25 Preterm, 8 Term-born, 8 Infants, 10 Adults, 7 17	(31.1–39.7 weeks) (1–14 days) (181–211 days) (24–31 years)	Global efficiency↑, clustering↓, modularity↓, small worldness ↓
Tymofiyeva O. et al. [25]	Characterize structural network topology in newborns with HIE	Newborn HIE	17	6 months	

**Table 2** (continued)

Study	Study purpose	Study population	Number	Age at scan Mean $\pm$ SD (range) Gender M/F	Findings
Jakab A. et al. 2015	To characterize structural brain networks in fetus with callosal agenesis	Fetuses	40 Fetuses, 20 Healthy control, 20	2nd trimester: GA 23.1 $\pm$ 1.2 weeks (22–25.3 weeks) 3rd trimester: GA 31 $\pm$ 3.3 weeks (26.3–36.3 weeks) 2nd trimester: GA 23.9 $\pm$ 1.1 weeks (22.4–25.8 weeks) 3rd trimester: GA 29.6 $\pm$ 2.5 weeks (25.8–33.5 weeks) Median age at enrollment, 2.4 years (1.1–5.1 years)	$\downarrow$ network integration and segregation with $\uparrow$ neuromotor deficit Less segregated nodes in acallosal brains and $\downarrow$ network centrality of thalamus and cingulate (hubs)
Englander Z.A. et al. [63]	To investigate connectivity changes throughout the brain in relation to functional outcomes in children with CP	Children with CP	17	Median age at enrollment, 2.4 years (1.1–5.1 years)	Strong correlation between increase in white matter connectivity and functional improvement
Pannek K. et al. [64]	Longitudinal study To identify pathways associated with unilateral CP from the structural network of connections	Children with unilateral CP	67 CP, 50 Healthy control, 17	Unilateral left CP, 10.5 $\pm$ 3 years (5.1–17) M/F, 11/12 Unilateral right CP, 11.4 $\pm$ 3.3 years (6–17.1) M/F, 15/12 Healthy control, 11.3 $\pm$ 2.7 years (7.7–16.3) M/F, 6/11 6.5 $\pm$ 4.5 years M/F, 6/4 5.9 $\pm$ 4.7 years	Altered structural connectivity including the corticospinal, thalamocortical, and fronto-parietal association pathways ( $\downarrow$ FA)
Meoded A. et al. [13]	To characterize the topological network measures and study connected and disconnected subnetworks in children with corpus callosum agenesis	Children <18 years with corpus callosum agenesis	20 CC agenesis, 10 Healthy controls, 10	6.5 $\pm$ 4.5 years M/F, 6/4 5.9 $\pm$ 4.7 years	Decreased global and increased local connectivity in CC agenesis. $\uparrow$ connectivity in interhemispheric and intrahemispheric subnetworks in CC agenesis $\downarrow$ connectivity in ASD in intra- and intersubnetwork connections in ASD group
Tunc B. et al. [65]	Identify subnetworks in children affected by autism spectrum disorders	Children with ASD	172 ASD, 97 Healthy controls, 75	12.6 $\pm$ 2.9 years 12.2 $\pm$ 3.3 years	$\downarrow$ connectivity in ASD in intra- and intersubnetwork connections in ASD group
Cao Q. et al. [66]	To determine whether patients with ADHD show disrupted topology efficiency and abnormal nodal/connectional properties in the whole brain WM	Children with ADHD	60 ADHD, 30 Healthy controls, 30	10.3 $\pm$ 1.9 years (8–14) 10.3 $\pm$ 1.6 (8–14)	$\downarrow$ structural connectivity in the prefrontal-dominant circuitry and $\uparrow$ connectivity in the orbitofrontal-striatal circuitry in ADHD

**Table 2** (continued)

Study	Study purpose	Study population	Number	Age at scan Mean $\pm$ SD (range) Gender M/F	Findings
Hong et al. [67]	networks and whether these changes are correlate with clinical behavioral To identify differences in brain network connectivity between ADHD subjects and controls and examine the functional effect of disrupted connectivity in ADHDH	Children and adolescents with ADHD	97 ADHD, 71 Healthy controls, 26	9.4 $\pm$ 2.6 years M/F, 56/15 10 $\pm$ 2.5 years M/F, 13/13	Changes correlated with the inattention and hyperactivity/impulsivity symptoms Aberrant networks involving prefrontal and striatal regions in ADHD subjects

M male, F female, GA gestational age, HIE hypoxic ischemic encephalopathy, CP cerebral palsy, CC corpus callosum, ASD autism spectrum disorders, ADHD attention-deficit/hyperactivity disorders

<sup>a</sup> Median corrected age

<sup>b</sup> Right-handed

<sup>c</sup> A subset of 28 preterm infants were scanned twice at 31 and 41 weeks

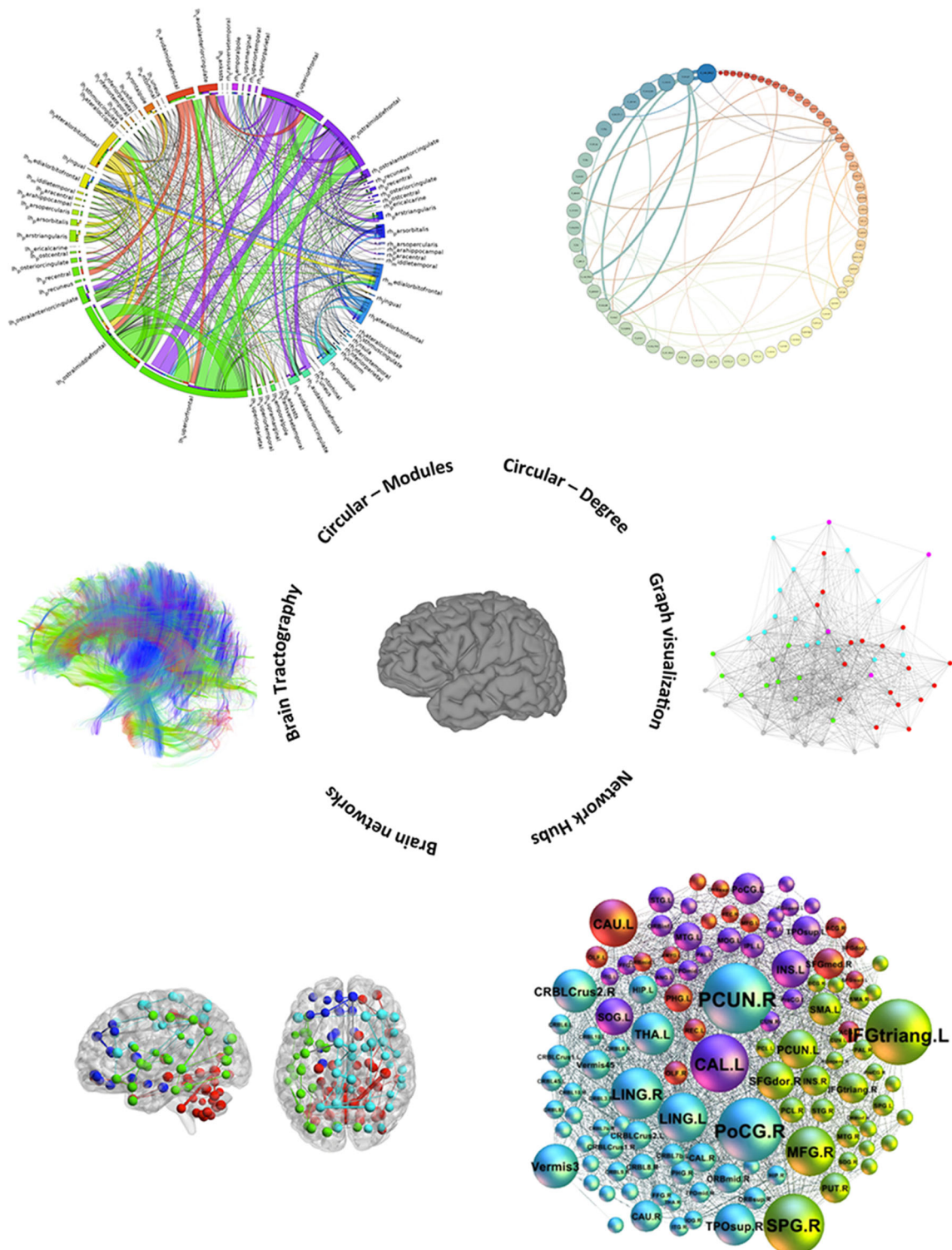


**Fig. 5** Visualization of the structural connectome and structural connectivity of a healthy 4-year boy, including (1) circular modules: all cortical regions depicted as *rectangles* with size based on degree of a module, connected by weighted edges; (2) circular degree: all cortical regions depicted as *circles* with size according to degree value; (3) graph visualization: network in nonanatomical space with different communities, *node color* represent assigned community; (4) network visualization

with nodes as spheres with *different colors and sizes*, according to modularity partitioning and hub, respectively; (5) networks in anatomical space: different modules are depicted with *different colors*, this type of visualization facilitates anatomical interpretation, but less optimal for dense networks; and (6) whole brain tractography, e.g., structural connectivity

groups and may be helpful in identifying alternate wiring or reorganization of brain networks [13].

### The whole picture—visualization of the structural connectome

The structure of the human brain is easily perceived by looking at two- or three-dimensional views. However, the increase interest and popularity in the human connectome have established a new neuroimaging dimension: the imaging of networks (Fig. 5). The analysis of the human connectome collects the connectivity of the human brain from multiple imaging modalities that are analyzed using graph theoretical techniques. The dimensionality of human connectivity data is high and the complex networks require sophisticated visualization and analysis software [77]. Innovations in data visualization punctuate the landmark advances in human connectome research since its origins including glyphs for DWI/DTI and graph-based brain network representations of structural connectivity data [78]. Connectome mapping has been a visual tale of increasing complexity, continuously oscillating between various priorities of data presentation. The result in any connectome visualization is a trade-off between of anatomical fidelity and connectome complexity. These challenges require balance between complexity and simplicity and between thoroughness and readability [78]. Finally, interactive connectome visualization tools are emerging. A representation of structural and functional connectomes using high-dimensional data followed by dimensionality reduction has been recently described. A “road map” of the human brain can be visualized using a novel visualization platform that reconstructs connectomes’ intrinsic geometry, implemented with virtual reality [79].

### Conclusion and future directions

In this review article, we outlined the different steps and the many challenges that remain in the acquisition, preprocessing, and analysis of the structural connectome in children. The measurement of the network topology allows a better understanding of the pathogenesis, implication for cognitive and behavioral functions, and treatment of pediatric brain disorders from a network perspective. Innovative methods of neuroimaging data analysis are essential for the structural connectome. Brain connectomics is becoming a core component of several neuroscience research projects. A fundamental challenge for all connectomics studies is the need for an efficient, robust, reliable, and easy-to-use pipeline to mine large neuroscience datasets [80]. State-of-the-art algorithms are currently being developed for mapping and analyzing the connectome. High performance clusters are being used for

the intensive computation involved in this type of analysis. Publicly available pipelines that such as MRImages to Graphs Pipeline will be used to map and analyze the patients’ connectome (M2G <http://openconnectome.org/graph-services/>). In conclusion, the human connectome provides an unparalleled compilation of neural data allowing navigating the brain and exploring developing brain circuits in a way that was not possible in the preconnectome era. Functional disorders including many behavioral and attention disorders may likely be better explored studying the internal networking.

**Acknowledgments** Data were provided in part by the Human Connectome Project, WU-Minn Consortium (Principal Investigators: David Van Essen and Kamil Ugurbil, 1U54MH091657) funded by the 16 NIH Institutes and Centers that support the NIH Blueprint for Neuroscience Research and by the McDonnell Center for Systems Neuroscience at Washington University.

### Compliance with ethical standards

**Funding** No funding was received for this study.

**Conflict of interest** The authors declare that they have no conflict of interest.

**Ethical approval** All procedures performed in the studies involving human participants were in accordance with the ethical standards of the institutional and/or national research committee and with the 1964 Helsinki Declaration and its later amendments or comparable ethical standards.

**Informed consent** This article includes human data that have been acquired for clinical indication; however, the Johns Hopkins Institutional Review Board issued a consent waiver for this study.

### References

- Craddock RC, Jbabdi S, Yan CG, Vogelstein JT, Castellanos FX, Di Martino A, Kelly C, Heberlein K, Colcombe S, Milham MP (2013) Imaging human connectomes at the macroscale. *Nat Methods* 10(6):524–539. doi:10.1038/nmeth.2482
- Sporns O, Tononi G, Kotter R (2005) The human connectome: a structural description of the human brain. *PLoS Comput Biol* 1(4):e42. doi:10.1371/journal.pcbi.0010042
- Bullmore E, Sporns O (2009) Complex brain networks: graph theoretical analysis of structural and functional systems. *Nat Rev Neurosci* 10(3):186–198. doi:10.1038/nrn2575
- Bullmore ET, Bassett DS (2011) Brain graphs: graphical models of the human brain connectome. *Annu Rev Clin Psychol* 7:113–140. doi:10.1146/annurev-clinpsy-040510-143934
- Erdos P, Renyi A (1960) On the evolution of random graphs. *B Int Statist Inst* 38(4):343–347
- Papo D, Buldu JM, Boccaletti S, Bullmore ET (2014) Complex network theory and the brain. *Philos Trans R Soc Lond Ser B Biol Sci* 369(1653). doi:10.1098/rstb.2013.0520
- Sporns O (2011) The human connectome: a complex network. *Ann N Y Acad Sci* 1224:109–125. doi:10.1111/j.1749-6632.2010.05888.x

8. Albert R, Barabasi AL (2002) Statistical mechanics of complex networks. *Rev Mod Phys* 74(1):47–97. doi:10.1103/Revmodphys.74.47
9. Bassett DS, Bullmore ET (2009) Human brain networks in health and disease. *Curr Opin Neurol* 22(4):340–347. doi:10.1097/WCO.0b013e32832d93dd
10. Latora V, Marchiori M (2001) Efficient behavior of small-world networks. *Phys Rev Lett* 87(19):198701. doi:10.1103/PhysRevLett.87.198701
11. Watts DJ, Strogatz SH (1998) Collective dynamics of ‘small-world’ networks. *Nature* 393(6684):440–442. doi:10.1038/30918
12. Sporns O, Zwi JD (2004) The small world of the cerebral cortex. *Neuroinformatics* 2(2):145–162. doi:10.1385/NI:2:2:145
13. Meoded A, Katipally R, Bosemani T, Huisman TA, Poretti A (2015) Structural connectivity analysis reveals abnormal brain connections in agenesis of the corpus callosum in children. *Eur Radiol* 25(5):1471–1478. doi:10.1007/s00330-014-3541-y
14. Owen JP, Li YO, Ziv E, Strominger Z, Gold J, Bukhpun P, Wakahiro M, Friedman EJ, Sherr EH, Mukherjee P (2013) The structural connectome of the human brain in agenesis of the corpus callosum. *NeuroImage* 70:340–355. doi:10.1016/j.neuroimage.2012.12.031
15. Widjaja E, Zamyadi M, Raybaud C, Snead OC, Doesburg SM, Smith ML (2015) Disrupted global and regional structural networks and subnetworks in children with localization-related epilepsy. *AJNR Am J Neuroradiol* 36(7):1362–1368. doi:10.3174/ajnr.A4265
16. Puetz VB, Parker D, Kohn N, Dahmen B, Verma R, Konrad K (2017) Altered brain network integrity after childhood maltreatment: a structural connectomic DTI-study. *Hum Brain Mapp* 38(2):855–868. doi:10.1002/hbm.23423
17. Ponsoda V, Martinez K, Pineda-Pardo JA, Abad FJ, Olea J, Roman FJ, Barbey AK, Colom R (2017) Structural brain connectivity and cognitive ability differences: a multivariate distance matrix regression analysis. *Hum Brain Mapp* 38(2):803–816. doi:10.1002/hbm.23419
18. Yuan W, Treble-Barna A, Sohlberg MM, Harn B, Wade SL (2017) Changes in structural connectivity following a cognitive intervention in children with traumatic brain injury. *Neurorehabil Neural Repair* 31(2):190–201. doi:10.1177/1545968316675430
19. Severino M, Tortora D, Toselli B, Uccella S, Traverso M, Morana G, Capra V, Veneselli E, Fato MM, Rossi A (2017) Structural connectivity analysis in children with segmental callosal agenesis. *AJNR Am J Neuroradiol*. doi:10.3174/ajnr.A5043
20. Jones DK (2004) The effect of gradient sampling schemes on measures derived from diffusion tensor MRI: a Monte Carlo study. *Magn Reson Med* 51(4):807–815. doi:10.1002/mrm.20033
21. Cammoun L, Gigandet X, Meskaldji D, Thiran JP, Sporns O, Do KQ, Maeder P, Meuli R, Hagmann P (2012) Mapping the human connectome at multiple scales with diffusion spectrum MRI. *J Neurosci Methods* 203(2):386–397. doi:10.1016/j.jneumeth.2011.09.031
22. Hagmann P, Sporns O, Madan N, Cammoun L, Pienaar R, Wedeen VJ, Meuli R, Thiran JP, Grant PE (2010) White matter maturation reshapes structural connectivity in the late developing human brain. *Proc Natl Acad Sci U S A* 107(44):19067–19072. doi:10.1073/pnas.1009073107
23. Hagmann P, Grant PE, Fair DA (2012) MR connectomics: a conceptual framework for studying the developing brain. *Front Syst Neurosci* 6:43. doi:10.3389/fnsys.2012.00043
24. Oishi K, Mori S, Donohue PK, Ernst T, Anderson L, Buchthal S, Faria A, Jiang H, Li X, Miller MI, van Zijl PC, Chang L (2011) Multi-contrast human neonatal brain atlas: application to normal neonate development analysis. *NeuroImage* 56(1):8–20. doi:10.1016/j.neuroimage.2011.01.051
25. Tymofiyeva O, Hess CP, Ziv E, Tian N, Bonifacio SL, McQuillen PS, Ferriero DM, Barkovich AJ, Xu D (2012) Towards the “baby connectome”: mapping the structural connectivity of the newborn brain. *PLoS One* 7(2):e31029. doi:10.1371/journal.pone.0031029
26. Zhu D, Li K, Guo L, Jiang X, Zhang T, Zhang D, Chen H, Deng F, Faraco C, Jin C, Wee CY, Yuan Y, Lv P, Yin Y, Hu X, Duan L, Hu X, Han J, Wang L, Shen D, Miller LS, Li L, Liu T (2013) DICCCOL: dense individualized and common connectivity-based cortical landmarks. *Cereb Cortex* 23(4):786–800. doi:10.1093/cercor/bhs072
27. Mori S, Zhang J (2006) Principles of diffusion tensor imaging and its applications to basic neuroscience research. *Neuron* 51(5):527–539. doi:10.1016/j.neuron.2006.08.012
28. Le Bihan D (1995) Molecular diffusion, tissue microdynamics and microstructure. *NMR Biomed* 8(7–8):375–386
29. Mori S, Crain BJ, Chacko VP, van Zijl PC (1999) Three-dimensional tracking of axonal projections in the brain by magnetic resonance imaging. *Ann Neurol* 45(2):265–269
30. Basser PJ, Mattiello J, LeBihan D (1994) MR diffusion tensor spectroscopy and imaging. *Biophys J* 66(1):259–267. doi:10.1016/S0006-3495(94)80775-1
31. Conturo TE, Lori NF, Cull TS, Akbudak E, Snyder AZ, Shimony JS, McKinstry RC, Burton H, Raichle ME (1999) Tracking neuronal fiber pathways in the living human brain. *Proc Natl Acad Sci U S A* 96(18):10422–10427
32. Pierpaoli C, Basser PJ (1996) Toward a quantitative assessment of diffusion anisotropy. *Magn Reson Med* 36(6):893–906
33. Pierpaoli C, Jezzard P, Basser PJ, Barnett A, Di Chiro G (1996) Diffusion tensor MR imaging of the human brain. *Radiology* 201(3):637–648. doi:10.1148/radiology.201.3.8939209
34. Hagmann P, Jonasson L, Maeder P, Thiran JP, Wedeen VJ, Meuli R (2006) Understanding diffusion MR imaging techniques: from scalar diffusion-weighted imaging to diffusion tensor imaging and beyond. *Radiographics* : a review publication of the Radiological Society of North America, Inc 26(Suppl 1):S205–S223. doi:10.1148/rg.26si065510
35. Tuch DS, Reese TG, Wiegell MR, Makris N, Belliveau JW, Wedeen VJ (2002) High angular resolution diffusion imaging reveals intravoxel white matter fiber heterogeneity. *Magn Reson Med* 48(4):577–582. doi:10.1002/mrm.10268
36. Basser PJ, Mattiello J, LeBihan D (1994) Estimation of the effective self-diffusion tensor from the NMR spin echo. *Journal of magnetic resonance Series B* 103(3):247–254
37. Wedeen VJ, Hagmann P, Tseng WY, Reese TG, Weisskoff RM (2005) Mapping complex tissue architecture with diffusion spectrum magnetic resonance imaging. *Magn Reson Med* 54(6):1377–1386. doi:10.1002/mrm.20642
38. Smith RE, Tournier JD, Calamante F, Connelly A (2012) Anatomically-constrained tractography: improved diffusion MRI streamlines tractography through effective use of anatomical information. *NeuroImage* 62(3):1924–1938. doi:10.1016/j.neuroimage.2012.06.005
39. Tournier JD, Calamante F, Connelly A (2007) Robust determination of the fibre orientation distribution in diffusion MRI: non-negativity constrained super-resolved spherical deconvolution. *NeuroImage* 35(4):1459–1472. doi:10.1016/j.neuroimage.2007.02.016
40. Sotiropoulos SN, Jbabdi S, Xu J, Andersson JL, Moeller S, Auerbach EJ, Glasser MF, Hernandez M, Sapiro G, Jenkinson M, Feinberg DA, Yacoub E, Lenglet C, Van Essen DC, Ugurbil K, Behrens TE (2013) Advances in diffusion MRI acquisition and processing in the Human Connectome Project. *NeuroImage* 80:125–143. doi:10.1016/j.neuroimage.2013.05.057
41. Irfanoglu MO, Modi P, Nayak A, Hutchinson EB, Sarlls J, Pierpaoli C (2015) DR-BUDDI (diffeomorphic registration for blip-up blip-down diffusion imaging) method for correcting echo planar

- imaging distortions. *NeuroImage* 106:284–299. doi:10.1016/j.neuroimage.2014.11.042
42. Berl MM, Walker L, Modi P, Irfanoglu MO, Sarlls JE, Nayak A, Pierpaoli C (2015) Investigation of vibration-induced artifact in clinical diffusion-weighted imaging of pediatric subjects. *Hum Brain Mapp*. doi:10.1002/hbm.22846
  43. Chang LC, Jones DK, Pierpaoli C (2005) RESTORE: robust estimation of tensors by outlier rejection. *Magn Reson Med* 53(5):1088–1095. doi:10.1002/mrm.20426
  44. Thomas C, Ye FQ, Irfanoglu MO, Modi P, Saleem KS, Leopold DA, Pierpaoli C (2014) Anatomical accuracy of brain connections derived from diffusion MRI tractography is inherently limited. *Proc Natl Acad Sci U S A* 111(46):16574–16579. doi:10.1073/pnas.1405672111
  45. Bastiani M, Shah NJ, Goebel R, Roebroeck A (2012) Human cortical connectome reconstruction from diffusion weighted MRI: the effect of tractography algorithm. *NeuroImage* 62(3):1732–1749. doi:10.1016/j.neuroimage.2012.06.002
  46. Gigandet X, Haggmann P, Kuran M, Cammoun L, Meuli R, Thiran JP (2008) Estimating the confidence level of white matter connections obtained with MRI tractography. *PLoS One* 3(12):e4006. doi:10.1371/journal.pone.0004006
  47. Prckovska V, Rodrigues P, Puigdemolliv Sanchez A, Ramos M, Andorra M, Martinez-Heras E, Falcon C, Prats-Galino A, Villoslada P (2015) Reproducibility of the structural connectome reconstruction across diffusion methods. *Journal of neuroimaging : official journal of the American Society of Neuroimaging*. doi:10.1111/jon.12298
  48. Rubinov M, Sporns O (2010) Complex network measures of brain connectivity: uses and interpretations. *NeuroImage* 52(3):1059–1069. doi:10.1016/j.neuroimage.2009.10.003
  49. Tymofiyeva O, Hess CP, Xu D, Barkovich AJ (2014) Structural MRI connectome in development: challenges of the changing brain. *Br J Radiol* 87(1039):20140086. doi:10.1259/bjr.20140086
  50. Cao M, Huang H, Peng Y, Dong Q, He Y (2016) Toward developmental connectomics of the human brain. *Front Neuroanat* 10:25. doi:10.3389/fnana.2016.00025
  51. Pandit AS, Robinson E, Aljabar P, Ball G, Gousias IS, Wang Z, Hajnal JV, Rueckert D, Counsell SJ, Montana G, Edwards AD (2014) Whole-brain mapping of structural connectivity in infants reveals altered connection strength associated with growth and preterm birth. *Cereb Cortex* 24(9):2324–2333. doi:10.1093/cercor/bht086
  52. Grayson DS, Ray S, Carpenter S, Iyer S, Dias TG, Stevens C, Nigg JT, Fair DA (2014) Structural and functional rich club organization of the brain in children and adults. *PLoS One* 9(2):e88297. doi:10.1371/journal.pone.0088297
  53. Kim DJ, Davis EP, Sandman CA, Sporns O, O'Donnell BF, Buss C, Hetrick WP (2014) Longer gestation is associated with more efficient brain networks in preadolescent children. *NeuroImage* 100:619–627. doi:10.1016/j.neuroimage.2014.06.048
  54. Yap PT, Fan Y, Chen Y, Gilmore JH, Lin W, Shen D (2011) Development trends of white matter connectivity in the first years of life. *PLoS One* 6(9):e24678. doi:10.1371/journal.pone.0024678
  55. Huang H, Shu N, Mishra V, Jeon T, Chalak L, Wang ZJ, Rollins N, Gong G, Cheng H, Peng Y, Dong Q, He Y (2015) Development of human brain structural networks through infancy and childhood. *Cereb Cortex* 25(5):1389–1404. doi:10.1093/cercor/bht335
  56. Baker ST, Lubman DI, Yucel M, Allen NB, Whittle S, Fulcher BD, Zalesky A, Fornito A (2015) Developmental changes in brain network hub connectivity in late adolescence. *J Neurosci* 35(24):9078–9087. doi:10.1523/JNEUROSCI.5043-14.2015
  57. Wierenga LM, van den Heuvel MP, van Dijk S, Rijks Y, de Reus MA, Durston S (2016) The development of brain network architecture. *Hum Brain Mapp* 37(2):717–729. doi:10.1002/hbm.23062
  58. Ball G, Aljabar P, Zebari S, Tusor N, Arichi T, Merchant N, Robinson EC, Ogundipe E, Rueckert D, Edwards AD, Counsell SJ (2014) Rich-club organization of the newborn human brain. *Proc Natl Acad Sci U S A* 111(20):7456–7461. doi:10.1073/pnas.1324118111
  59. Zhao T, Cao M, Niu H, Zuo XN, Evans A, He Y, Dong Q, Shu N (2015) Age-related changes in the topological organization of the white matter structural connectome across the human lifespan. *Hum Brain Mapp* 36(10):3777–3792. doi:10.1002/hbm.22877
  60. Chen Z, Liu M, Gross DW, Beaulieu C (2013) Graph theoretical analysis of developmental patterns of the white matter network. *Front Hum Neurosci* 7:716. doi:10.3389/fnhum.2013.00716
  61. Koenis MM, Brouwer RM, van den Heuvel MP, Mandl RC, van Soelen IL, Kahn RS, Boomsma DI, Hulshoff Pol HE (2015) Development of the brain's structural network efficiency in early adolescence: a longitudinal DTI twin study. *Hum Brain Mapp* 36(12):4938–4953. doi:10.1002/hbm.22988
  62. Tymofiyeva O, Hess CP, Ziv E, Lee PN, Glass HC, Ferriero DM, Barkovich AJ, Xu D (2013) A DTI-based template-free cortical connectome study of brain maturation. *PLoS One* 8(5):e63310. doi:10.1371/journal.pone.0063310
  63. Englander ZA, Sun J, Laura C, Mikati MA, Kurtzberg J, Song AW (2015) Brain structural connectivity increases concurrent with functional improvement: evidence from diffusion tensor MRI in children with cerebral palsy during therapy. *Neuroimage Clin* 7:315–324. doi:10.1016/j.nicl.2015.01.002
  64. Pannek K, Boyd RN, Fiori S, Guzzetta A, Rose SE (2014) Assessment of the structural brain network reveals altered connectivity in children with unilateral cerebral palsy due to periventricular white matter lesions. *Neuroimage Clin* 5:84–92. doi:10.1016/j.nicl.2014.05.018
  65. Tunc B, Shankar V, Parker D, Schultz RT, Verma R (2015) Towards a quantified network portrait of a population. *Inf Process Med Imaging* 24:650–661
  66. Cao Q, Shu N, An L, Wang P, Sun L, Xia MR, Wang JH, Gong GL, Zang YF, Wang YF, He Y (2013) Probabilistic diffusion tractography and graph theory analysis reveal abnormal white matter structural connectivity networks in drug-naive boys with attention deficit/hyperactivity disorder. *J Neurosci* 33(26):10676–10687. doi:10.1523/JNEUROSCI.4793-12.2013
  67. Hong SB, Zalesky A, Fornito A, Park S, Yang YH, Park MH, Song IC, Sohn CH, Shin MS, Kim BN, Cho SC, Han DH, Cheong JH, Kim JW (2014) Connectomic disturbances in attention-deficit/hyperactivity disorder: a whole-brain tractography analysis. *Biol Psychiatry* 76(8):656–663. doi:10.1016/j.biopsych.2013.12.013
  68. Girvan M, Newman ME (2002) Community structure in social and biological networks. *Proc Natl Acad Sci U S A* 99(12):7821–7826. doi:10.1073/pnas.122653799
  69. Newman ME (2004) Fast algorithm for detecting community structure in networks. *Phys Rev E Stat Nonlinear Soft Matter Phys* 69(6 Pt 2):066133. doi:10.1103/PhysRevE.69.066133
  70. Brandes U (2001) A faster algorithm for betweenness centrality. *J Math Sociol* 25(2):163–177
  71. Freeman LC (1979) Centrality in social networks conceptual clarification. *Soc Networks* 1(3):215–239. doi:10.1016/0378-8733(78)90021-7
  72. Newman MEJ (2002) Assortative mixing in networks. *Phys Rev Lett* 89(20). doi:10.1103/PhysRevLett.89.208701
  73. Bassett DS, Bullmore E (2006) Small-world brain networks. *The Neuroscientist : a review journal bringing neurobiology, neurology and psychiatry* 12(6):512–523. doi:10.1177/1073858406293182
  74. Sporns O, Honey CJ (2006) Small worlds inside big brains. *Proc Natl Acad Sci U S A* 103(51):19219–19220. doi:10.1073/pnas.0609523103

75. Tononi G, Sporns O, Edelman GM (1994) A measure for brain complexity: relating functional segregation and integration in the nervous system. *Proc Natl Acad Sci U S A* 91(11):5033–5037
76. Zalesky A, Fornito A, Bullmore ET (2010) Network-based statistic: identifying differences in brain networks. *NeuroImage* 53(4):1197–1207. doi:[10.1016/j.neuroimage.2010.06.041](https://doi.org/10.1016/j.neuroimage.2010.06.041)
77. LaPlante RA, Douw L, Tang W, Stufflebeam SM (2014) The connectome visualization utility: software for visualization of human brain networks. *PLoS One* 9(12):e113838. doi:[10.1371/journal.pone.0113838](https://doi.org/10.1371/journal.pone.0113838)
78. Margulies DS, Bottger J, Watanabe A, Gorgolewski KJ (2013) Visualizing the human connectome. *NeuroImage* 80:445–461. doi:[10.1016/j.neuroimage.2013.04.111](https://doi.org/10.1016/j.neuroimage.2013.04.111)
79. Ye AQ, Ajilore OA, Conte G, GadElkarim J, Thomas-Ramos G, Zhan L, Yang S, Kumar A, Magin RL, Forbes AG, Leow AD (2015) The intrinsic geometry of the human brain connectome. *Brain Inform* 2(4):197–210. doi:[10.1007/s40708-015-0022-2](https://doi.org/10.1007/s40708-015-0022-2)
80. A XT (2015) Connectome computation system for discovery science of brain. *Science Bulletin*